

A Finite-time Particle Swarm Optimization Algorithm

Qiang Lu and Qing-Long Han*

Centre for Intelligent and Networked Systems

School of Information and Communication Technology

Central Queensland University, Rockhampton, QLD 4702, Australia

*Corresponding author: Tel. +61 7 4930 9270

Email: {q.lu, q.han}@cqu.edu.au

Abstract—This paper deals with a class of optimization problems by designing and analyzing a finite-time particle swarm optimization (FPSO) algorithm. Two versions of the FPSO algorithm, which consist of a continuous-time FPSO algorithm and a discrete-time FPSO algorithm, are proposed. Firstly, the continuous-time FPSO algorithm is derived from the continuous model of the particle swarm optimization (PSO) algorithm by introducing a nonlinear damping item that can enable the continuous-time FPSO algorithm to converge within a finite-time interval and a parameter that can enhance the exploration capability of the continuous-time FPSO algorithm. Secondly, the corresponding discrete-time version of the FPSO algorithm is proposed by employing the same discretization scheme as the generalized particle swarm optimization (GPSO) such that the exploiting capability of the discrete-time FPSO algorithm is improved. Thirdly, a Lyapunov approach is used to analyze the finite-time convergence of the continuous-time FPSO algorithm and the stability region of the discrete-time FPSO algorithm is also given. Finally, the performance capabilities of the proposed discrete-time FPSO algorithm are illustrated by using three well-known benchmark functions (global minimum surrounded by multiple minima): Griewank, Rastrigin, and Ackley. In terms of numerical simulation results, the proposed continuous-time FPSO algorithm is used to deal with the problem of odor source localization by coordinating a group of robots.

I. INTRODUCTION

In the last decade, particle swarm optimization (PSO) as a kind of swarm intelligence techniques has been widely studied [12], [14]. Empirical evidences have been accumulated to show that PSO is a useful tool for optimization problems [14]. Due to lacking precision in a local search solution, an inertia factor ω in the velocity updating equation is introduced into the original version of PSO [5], [10], which gives rise to a commonly used form of PSO described by

$$\begin{aligned} \mathbf{v}_i(k+1) &= f(\mathbf{v}_i(k), \mathbf{u}_i(k)) \\ \mathbf{x}_i(k+1) &= \mathbf{x}_i(k) + \mathbf{v}_i(k+1) \end{aligned} \quad (1)$$

with

$$f(\mathbf{v}_i(k), \mathbf{u}_i(k)) = \omega \mathbf{v}_i(k) + \mathbf{u}_i(k) \quad (2)$$

$$\mathbf{u}_i(k) = \alpha_1(\mathbf{x}_l(k) - \mathbf{x}_i(k)) + \alpha_2(\mathbf{x}_g(k) - \mathbf{x}_i(k)) \quad (3)$$

where $\mathbf{v}_i(k) = (v_1(k) \ v_2(k) \ \cdots \ v_n(k))^T$ ($i = 1, 2, \dots, N$) is a velocity vector; $\mathbf{u}_i(k)$ is a control vector;

$\mathbf{x}_l(k)$ denotes previously best position of the i^{th} particle; $\mathbf{x}_g(k)$ refers to the globally best position of the swarm; ω is the inertia factor; N is the number of particles; $f: R^n \times R^n \rightarrow R^n$ is a map and α_j ($j = 1, 2$) is a random parameter, called acceleration coefficient.

The study of the PSO algorithm generally falls into two categories, namely, performance improvement [7], [11] and stability analysis [2], [8], [10]. For performance improvement, the PSO algorithm is modified based on the characteristics of optimization problems such that it can efficiently deal with a class of optimization problems, e.g. the problem of odor source localization [11] and the problem of vertical electrical sounding [7]. For stability analysis, several tools from the linear system theory and nonlinear system theory, such as a Lyapunov approach and a passivity approach, are used to analyze the convergence of a particle swarm [2], [8], [10]. It is worth mentioning that, given a control law $\mathbf{u}_i(k)$ in (3), current stability analysis in the references [2], [8], [10] can guarantee the convergence of the particle swarm under several assumption conditions when $k \rightarrow \infty$, that is, the references [2], [8], [10] describe several asymptotically stable conditions for the particle swarm.

There exists a class of optimization problems, which is a type of ill-posedness (a global maximum surrounded by multiple maxima) and usually requires the designed PSO algorithm to satisfy several conditions, such as accurate localization and robustness against uncertainties. In other words, from the aspect of performance improvement, the designed PSO algorithm is required to enhance its exploration capability and robustness against uncertainties; On the other hand, from the aspect of stability analysis, the designed PSO algorithm converges within a finite-time interval such that it can adapt the position magnitude to accurately locate the optimum [7]. It should be pointed out that odor source localization belongs to this class of optimization problems, which is stated in [11]. For the problem of odor source localization, the multi-robot system repeats to perform the process of “prediction-localization-prediction” in order to search for the odor source. Accordingly, the designed PSO algorithm coordinates multiple robots to predict the position of odor source through swarm information and individual information. And then, at the localization process, the multi-robot system will explore and

exploit the search space to trace the odor clues. Finally, within a finite-time interval, the multi-robot system will accurately locate the target position. Therefore, in order to guarantee the finite-time convergence of the particle swarm and to enhance the search ability for the class of optimization problems, how to design a finite-time control law $u_i(k)$ in (1), i.e., how to develop a finite-time particle swarm optimization algorithm is the motivation of the current study.

Due to several advantages including higher control accuracy, better disturbance rejection and robustness against uncertainties [1], the design of finite-time controllers for the system of multiple agents has received a growing interest from researchers and engineers [3], [15]. The idea in this paper is in part from the work on the design of finite-time controllers for the multi-robot system [3], [15] and from the study of swarming behaviors [4], [13]. Hence, we will first propose a continuous-time FPSO algorithm, which is derived from the continuous model of the PSO algorithm by introducing a nonlinear damping item that can enable the continuous-time FPSO algorithm to converge within a finite-time interval and a parameter that can enhance the exploration capability of the continuous-time FPSO algorithm. Then, we will propose a discrete-time FPSO algorithm, which is obtained by using the same discretization scheme as the GPSO algorithm [9]. Next, we will analyze the finite-time convergence of the continuous-time FPSO algorithm by employing a Lyapunov approach and give a convergence region of the discrete-time FPSO algorithm. Finally, we will illustrate the performance capabilities of the discrete-time FPSO algorithm in terms of three well-known benchmark functions (global minimum surrounded by multiple minima): Griewank, Rastrigin, and Ackley. In terms of the results of the numerical simulation, we will use the continuous-time FPSO algorithm to deal with the problem of odor source localization by coordinating a multi-robot system.

Notation: l_N denotes the index set $\{1, 2, \dots, N\}$. Let $\text{sig}(r)^a = \text{sign}(r)|r|^a$, where $0 < a < 1$, $r \in \mathbb{R}$, and $\text{sign}(\cdot)$ is the sign function.

II. THE CONTINUOUS MODEL OF THE PSO ALGORITHM

In this section, we will briefly describe the continuous model of the PSO algorithm, which will be used to derive the FPSO algorithm in the later section. Since the dynamics of each dimension of particles is independent of others, we assume that $n = 1$ without loss of generality in the following. Therefore, the stochastic differential model of the PSO algorithm, i.e. the continuous model of the PSO algorithm, can be given as

$$\ddot{x}_i(t) + (1 - \omega)\dot{x}_i(t) + \alpha x_i(t) = \alpha_1 x_l(t) + \alpha_2 x_g(t) \quad (4)$$

with

$$\begin{aligned} \alpha &= \alpha_1 + \alpha_2 \\ x_i(0) &= x_0 \\ \dot{x}_i(0) &= v_0 \end{aligned}$$

where $x_i(t)$ and $x_g(t)$ are the trajectories of the local and global best positions associated with the i^{th} ($i \in l_N$) particle, respectively; α_j ($j = 1, 2$) is a random variable; $x_i(0)$ and $\dot{x}_i(0)$ are the initial states at time $t = 0$.

This continuous PSO model is derived by Fernández Martínez *et al.* [9] (2008) in terms of physical analogy with a damped mass-spring oscillator. We use the following discretization scheme in (5), and then introduce it into the stochastic differential model of the PSO algorithm in (4).

$$\begin{aligned} \dot{x}_i(t) &\simeq \frac{x_i(t) - x_i(t - \Delta t)}{\Delta t} \\ \ddot{x}_i(t) &\simeq \frac{x_i(t + \Delta t) - 2x_i(t) + x_i(t - \Delta t)}{\Delta t^2} \end{aligned} \quad (5)$$

In one case that is $\Delta t = 1$ and $t = k$, we have

$$\begin{aligned} x(k+1) &= -(\alpha - \omega - 1)x(k) - \omega x(k-1) \\ &\quad + \alpha_1 x_l(k) + \alpha_2 x_g(k) \end{aligned} \quad (6)$$

with

$$\begin{aligned} x_i(0) &= x_0 \\ x_i(1) &= (1 - \alpha)x_0 + \omega v_0 \\ &\quad + \alpha_1 x_l(0) + \alpha_2 x_g(0) \end{aligned}$$

It is worth noting that the difference form of the PSO algorithm in (6) can be rewritten in terms of the position and velocity. Consequently, we can derive the most commonly used form, which is presented by (1).

In another case that is $\Delta t > 0$, the GPSO algorithm [7] can be obtained as

$$\begin{aligned} x_i(t + \Delta t) &= \gamma_1 x_i(t) + \gamma_2 x_i(t - \Delta t) \\ &\quad + \Delta t^2 (\alpha_1 x_l(k) + \alpha_2 x_g(k)) \end{aligned} \quad (7)$$

with

$$\begin{aligned} \gamma_1 &= 2 - (1 - \omega)\Delta t - \alpha\Delta t^2 \\ \gamma_2 &= (1 - \omega)\Delta t - 1 \end{aligned}$$

We rewrite the equation (7) based on the position and velocity ($x_i(t), v_i(t)$) as

$$\begin{aligned} v_i(t + \Delta t) &= (1 - (1 - \omega)\Delta t)v_i(t) \\ &\quad + \alpha\Delta t \left(\frac{\alpha_1 x_l(t) + \alpha_2 x_g(t)}{\alpha_1 + \alpha_2} - x_i(t) \right) \\ x_i(t + \Delta t) &= x_i(t) + v_i(t + \Delta t)\Delta t \end{aligned} \quad (8)$$

As pointed out by Fernández Martínez *et al.* [9] (2008), the particle swarm movement controlled by the GPSO algorithm becomes more elastic and less damped when $\Delta t \rightarrow 0$.

III. A FINITE-TIME PSO ALGORITHM

In this section, according to the continuous model of the PSO algorithm, we will first give a continuous-time FPSO algorithm, and then present remarks about parameters introduced by the continuous-time FPSO algorithm. Finally, we will derive a discrete-time FPSO algorithm.

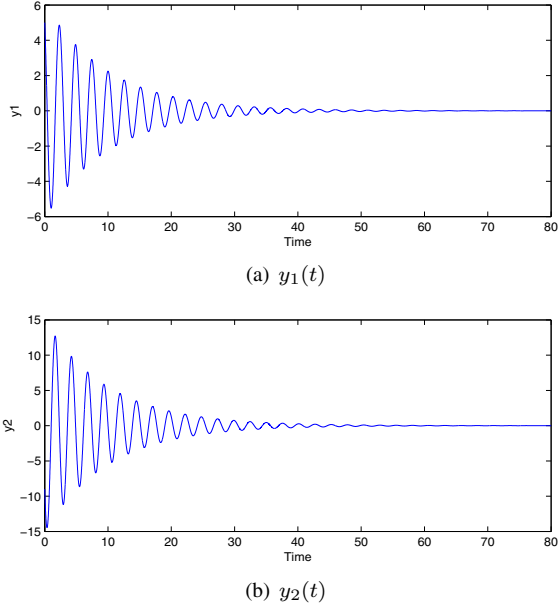


Fig. 1. The convergence curves of the system states in (11) ($\omega = 0.8$, $\alpha = 6$, $y_1(0) = 5$, and $y_2(0) = -9$).

A. A Continuous-time Model of the FPSO Algorithm

We introduce the oscillation center $p_i(t)$ as

$$p_i(t) = \frac{\alpha_1 x_l(t) + \alpha_2 x_g(t)}{\alpha_1 + \alpha_2} \quad (9)$$

Let $\xi_i(t) = x_i(t) - p_i(t)$ and introduce $\xi_i(t)$ into the continuous model of the PSO algorithm in (4). We have

$$\ddot{\xi}_i(t) + (1 - \omega)\dot{\xi}_i(t) + \alpha\xi_i(t) = -\ddot{p}_i(t) - (1 - \omega)\dot{p}_i(t) \quad (10)$$

Moreover, set $y_1(t) = \xi_i(t)$ and $y_2(t) = \dot{\xi}_i(t)$. Then, the equation (10) is rewritten as

$$\begin{aligned} \dot{y}_1(t) &= y_2(t) \\ \dot{y}_2(t) &= -(1 - \omega)y_2(t) - \alpha y_1(t) \\ &\quad - (1 - \omega)\dot{p}_i(t) - \ddot{p}_i(t) \end{aligned} \quad (11)$$

In the stagnation case ($p_i(t)$ is stable), the system described by (11) is asymptotically stable at the origin when $t \rightarrow \infty$, if the parameters ω and α satisfy $\omega < 1$ and $\alpha > 0$, respectively. Figure 1 illustrates the asymptotical stability of the system given by (11).

In what follows, we first present the definition of the finite-time stability [1].

Definition 1: Consider the system $\dot{\mathbf{y}} = f(\mathbf{y}(t))$. The origin is said to be a finite-time-stable equilibrium if there exists an open neighborhood $\mathcal{N} \subseteq \mathcal{D}$ of the origin and a function $T : \mathcal{N} \setminus \{0\} \rightarrow (0, \infty)$, such that for every $\mathbf{y}_0 \in \mathcal{N} \setminus \{0\}$, $\mathbf{y}(t)$ is defined for $t \in [0, T(\mathbf{y}_0)]$, $\mathbf{y}(t) \in \mathcal{N} \setminus \{0\}$, for $t \in [0, T(\mathbf{y}_0)]$, and $\lim_{t \rightarrow T(\mathbf{y}_0)} \mathbf{y}(t) = \mathbf{0}$. If $\mathcal{D} = \mathcal{N} = \mathbb{R}^n$, the origin is said to be a globally finite-time-stable equilibrium.

Next, we provide a nonlinear finite-time PSO algorithm. In order to enable the states of the system (11) to fast converge to the origin and enlarge the magnitude of state oscillation, a

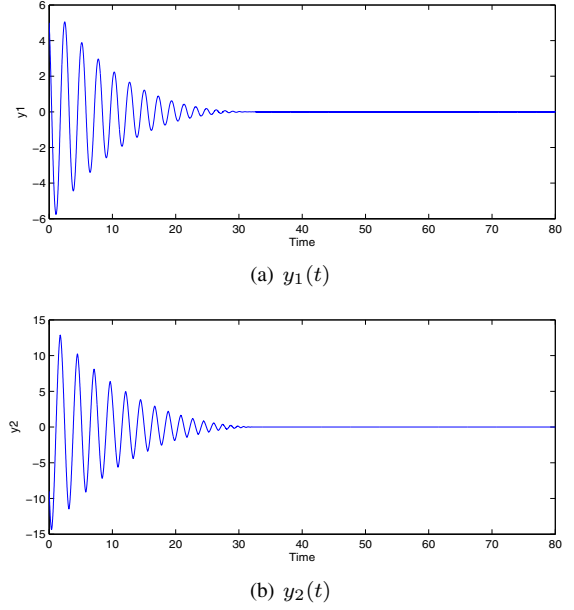


Fig. 2. The convergence curves of the system states in (12) ($\omega = 0.8$, $\alpha = 6$, $a = 0.5$, $\beta = 1.9$, $\gamma = 0.5$, $y_1(0) = 5$, and $y_2(0) = -9$).

nonlinear damping item and a parameter γ are added into the system (11) as:

$$\begin{aligned} \dot{y}_1(t) &= y_2(t) \\ \dot{y}_2(t) &= -\gamma \left((1 - \omega)y_2(t) + \alpha y_1(t) \right) \\ &\quad - \beta \text{sig} \left((1 - \omega)y_2(t) + \alpha y_1(t) \right)^a \\ &\quad - \gamma(1 - \omega)\dot{p}_i(t) - \ddot{p}_i(t) \end{aligned} \quad (12)$$

where $0 < a < 1$, $\beta > 0$, and $0 < \gamma \leq 1$.

It is obvious that if $\beta = 0$ and $\gamma = 1$, then the system described by (12) becomes a linear system (11), which was studied by Fernández Martínez *et al.* [9] (2008). Hence, the system (11) can be regarded as a special case of the system (12). Figure 2 illustrates the convergence of the system states in (12) under the same parameter values ω , α and initial states $y_1(0)$, $y_2(0)$ in the stagnation case.

By letting $y_1(t) = \xi_i(t)$ and $y_2(t) = \dot{\xi}_i(t)$, the system (12) can be written as

$$\begin{aligned} \ddot{\xi}_i(t) + \gamma(1 - \omega)\dot{\xi}_i(t) &= -\gamma\alpha\xi_i(t) \\ &\quad - \beta \text{sig} \left((1 - \omega)\dot{\xi}_i(t) + \alpha\xi_i(t) \right)^a \\ &\quad - \ddot{p}_i(t) - \gamma(1 - \omega)\dot{p}_i(t) \end{aligned} \quad (13)$$

Moreover, by setting $\xi_i(t) = x_i(t) - p_i(t)$, the continuous-

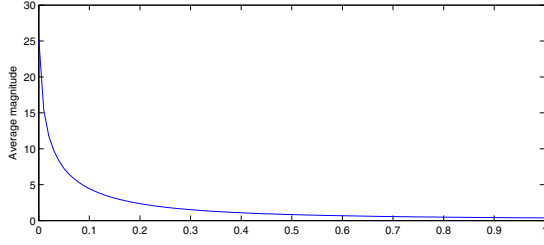


Fig. 3. The curve of the average oscillation magnitude for the parameter γ for the system state $y_2(t)$ in (12) ($\omega = 0.8$, $\alpha = 6$, $a = 0.5$, $\beta = 0.1$, $y_1(0) = 5$, and $y_2(0) = -9$).

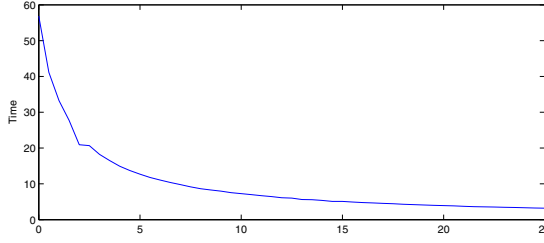


Fig. 4. The curve of the convergence time for the parameter β for the system state $y_2(t)$ in (12) ($\omega = 0.8$, $\alpha = 6$, $a = 0.5$, $\gamma = 1$, $y_1(0) = 5$, and $y_2(0) = -9$).

time FPSO algorithm is presented by

$$\begin{aligned} \ddot{x}_i(t) + \gamma(1 - \omega)\dot{x}_i(t) &= -\gamma\alpha(x_i(t) - p_i(t)) \\ &\quad - \beta \text{sig} \left((1 - \omega)(\dot{x}_i(t) - \dot{p}_i(t)) \right. \\ &\quad \left. + \alpha(x_i(t) - p_i(t)) \right)^a \end{aligned} \quad (14)$$

The continuous model of the FPSO algorithm is a globally finite-time stable, if the five parameters ($\omega, \alpha, a, \gamma, \beta$) fall into the following set (15), which will be proved in the next section.

$$\Omega_c = \{(\omega, \alpha, a, \gamma, \beta) : \omega < 1, \alpha > 0, 0 < a < 1, 0 < \gamma \leq 1, \beta > 0\} \quad (15)$$

It should be pointed out that the parameters γ and β can control the oscillation magnitude and the convergence speed of the state trajectory of the particle, respectively. Decreasing the parameter γ means the increase of average oscillation magnitude while increasing the parameter β means the decrease of the convergence time, which is shown in Fig.3 and Fig.4, respectively. Therefore, the proposed continuous-time FPSO algorithm can provide a flexible mechanism to control “elasticity” and “magnitude” such that this algorithm can efficiently control the particle swarm to explore the optimum, exploit the optimum, and locate the optimum.

B. A Discrete-time Model of the FPSO Algorithm

We discretize the system (14) to derive the discrete-time model of the FPSO algorithm by employing (5) and

$$\dot{p}_i(t) \simeq \frac{p_i(t) - p(t - \Delta t)}{\Delta t} \quad (16)$$

The discrete model is described by

$$\begin{aligned} x_i(t + \Delta t) &= \gamma_1 x_i(t) + \gamma_2 x_i(t - \Delta t) \\ &\quad + \gamma \Delta t^2 \alpha p_i(t) \\ &\quad - \beta \text{sig} \left(\gamma_3 x_i(t) - \gamma_3 p_i(t) \right. \\ &\quad \left. - \gamma_4 x_i(t - \Delta t) + \gamma_4 p_i(t - \Delta t) \right)^a \end{aligned} \quad (17)$$

with

$$\begin{aligned} \gamma_1 &= 2 - \gamma(1 - \omega)\Delta t - \gamma\alpha\Delta t^2 \\ \gamma_2 &= \gamma(1 - \omega)\Delta t - 1 \\ \gamma_3 &= (1 - \omega)\Delta t^{\frac{2-a}{a}} + \alpha\Delta t^{\frac{2}{a}} \\ \gamma_4 &= (1 - \omega)\Delta t^{\frac{2-a}{a}} \end{aligned}$$

Based on the forms of the position and velocity, the discrete-time model of the FPSO algorithm is given by

$$\begin{aligned} v_i(t + \Delta t) &= (1 - \gamma(1 - \omega)\Delta t)v_i(t) \\ &\quad + \gamma\alpha\Delta t(p_i(t) - x_i(t)) \\ &\quad - \beta \text{sig} \left(\gamma_8 x_i(t) - \gamma_5 p_i(t) \right. \\ &\quad \left. + \gamma_7 v_i(t) + \gamma_6 p_i(t - \Delta t) \right)^a \\ x_i(t + \Delta t) &= x_i(t) + v_i(t + \Delta t)\Delta t \end{aligned} \quad (18)$$

with

$$\begin{aligned} \gamma_5 &= (1 - \omega)\Delta t^{\frac{1-a}{a}} + \alpha\Delta t^{\frac{1}{a}} \\ \gamma_6 &= (1 - \omega)\Delta t^{\frac{1-a}{a}} \\ \gamma_7 &= (1 - \omega)\Delta t^{\frac{1}{a}} \\ \gamma_8 &= \alpha\Delta t^{\frac{1}{a}} \end{aligned}$$

In order to illustrate the convergence of the position and velocity for the discrete PSO algorithm, the GPSO algorithm and the discrete-time FPSO algorithm, respectively, we set $p_i(t) = 0$. The corresponding results can be seen in Fig.5, Fig.6, and Fig.7. From Fig.5 (b) and Fig.6 (b), one can see that the position change for the GPSO algorithm becomes more elastic and there exist more sampling points than the discrete PSO algorithm. But, the magnitude of position oscillation for the GPSO algorithm is smaller than that of position oscillation for the discrete-time PSO algorithm, which can result in a weak exploration for the search space. It is worth mentioning that the discrete-time FPSO algorithm provides a mechanism, that is, the attenuation of swarm movement and the magnitude of position oscillation are controllable through adjusting the

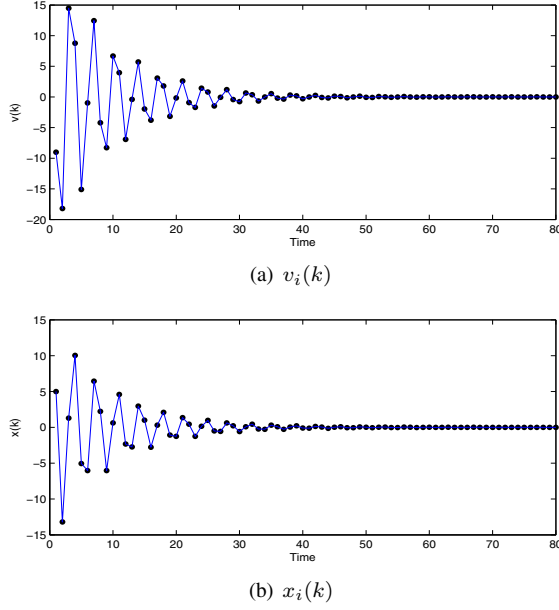


Fig. 5. The convergence curves of the states of the basic model of the discrete PSO ($\omega = 0.8$, $\alpha = 2.2$, $\beta = 0$, $\gamma = 1$, $\Delta t = 1$, $x_i(0) = 5$, and $v_i(0) = -9$).

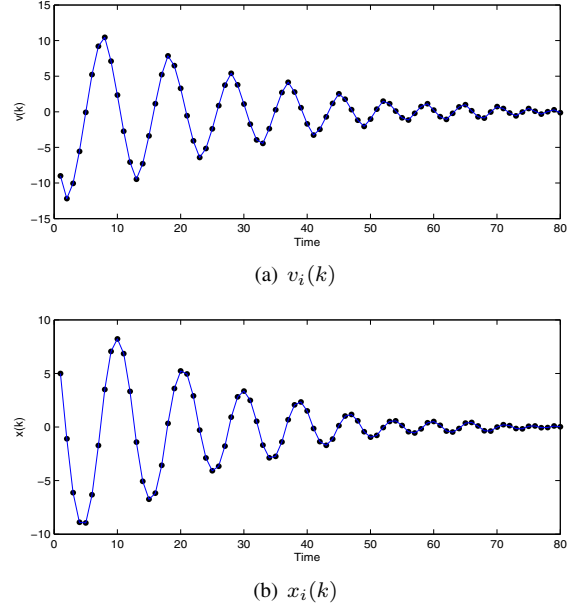


Fig. 7. The convergence curves of the states of the finite-time model of the discrete PSO ($\omega = 0.8$, $\alpha = 2.2$, $\beta = 0.5$, $\gamma = 0.5$, $\Delta t = 0.5$, $x_i(0) = 5$, and $v_i(0) = -9$).

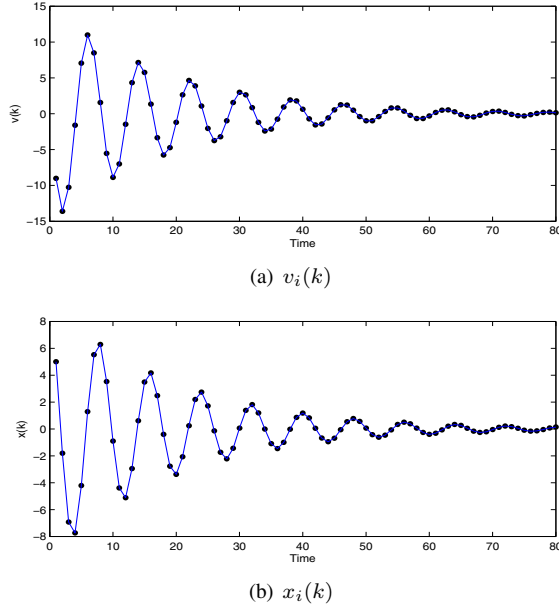


Fig. 6. The convergence curves of the states of the generalized model of the discrete PSO ($\omega = 0.8$, $\alpha = 2.2$, $\beta = 0$, $\gamma = 1$, $\Delta t = 0.5$, $x_i(0) = 5$, and $v_i(0) = -9$).

parameters β and γ , which can be seen in Fig.7 (b). Therefore, the proposed discrete-time FPSO algorithm provides a flexible tool for a class of optimization problems.

Remark 1: In this paper, we only consider the stagnation case. For the moving center $p_i(t)$, we will deal with it in the near future.

IV. STABILITY ANALYSIS

In this section, we will prove the finite-time stability of the continuous-time model of the FPSO algorithm and give a convergence region of the discrete-time model of the FPSO algorithm. Before giving the convergence proof, we have the following lemma [1].

Lemma 1: Suppose there exists a continuously differentiable function $V : \mathcal{D} \rightarrow \mathbb{R}$, real number $k > 0$ and $a \in (0, 1)$, and a neighborhood $\mathcal{U} \subset \mathcal{D}$ of the origin such that V is positive definite on \mathcal{U} and $\dot{V} + kV^a$ is negative semidefinite on \mathcal{U} . Then the origin is a finite-time-stable equilibrium of the system $\dot{\mathbf{y}} = f(\mathbf{y}(t))$. Moreover, if T is the settling time, then $T(\mathbf{y}_0) \leq \frac{1}{k(1-a)} V(\mathbf{y}_0)^{1-a}$ for all \mathbf{y}_0 in the open neighborhood of the origin.

Proof: This proof can be found in [1]. \square

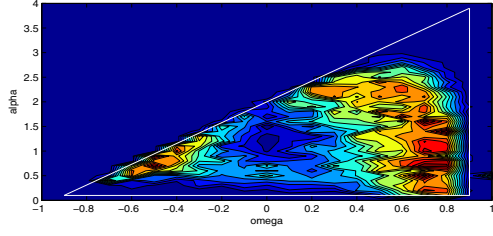
Based on the Lemma 1, Lyapunov analysis provides the following global convergence result.

Theorem 1: Consider the continuous-time model of the FPSO algorithm (14) with $(\omega, \alpha, a, \gamma, \beta) \in \Omega_c$ in (15). If the oscillation center $p_i(t)$ is stable in the stagnation case, i.e. $p_i(t) = p^*$, then the p^* is a globally finite-time-stable equilibrium of the continuous-time model of the FPSO algorithm (14). Moreover, the continuous FPSO algorithm converges within a finite-time interval $\left[0, \frac{(1+a)V(0)^{\frac{1-a}{1+a}}}{k(1-a)}\right]$.

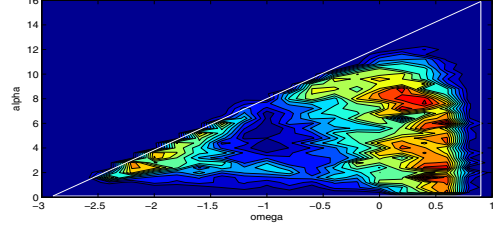
Proof: This theorem is proven through the following two steps.

Step 1: Transfer the equilibrium p^* of the system (14) to the origin.

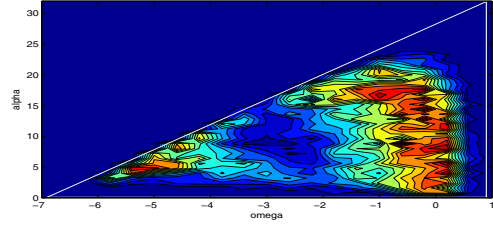
Introduce $\xi_i(t) = x_i(t) - p_i(t)$ into (14) and set $y_1(t) = \xi_i(t)$, $y_2(t) = \xi_i(t)$. Hence, we can obtain the system (12).



(a) PSO



(b) GPSO $\Delta t = 0.5$



(c) FPSO $\Delta t = 0.5, \gamma = 0.5, \beta = 0.01$

Fig. 8. Success rates for the Griewank function for PSO, GPSO, and FPSO.

Since the $p_i(t)$ is stable in the stagnation case, the system (12) can be written as

$$\begin{aligned}\dot{y}_1(t) &= y_2(t) \\ \dot{y}_2(t) &= -\gamma\phi_a - \beta\text{sig}(\phi_a)^a\end{aligned}\quad (19)$$

for every $a \in (0, 1)$, where $\phi_a = (1 - \omega)y_2(t) + \alpha y_1(t)$.

If the origin $(0, 0)$ of the system (19) is a finite-time-stable equilibrium, $x_i(t)$ will reach p^* in finite-time.

Step 2: Choose a Lyapunov candidate as

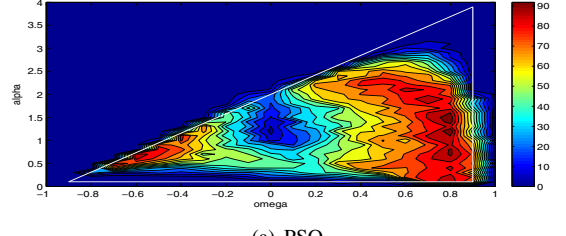
$$\begin{aligned}V(t) &= \frac{\beta(1-\omega)}{a+1}|\phi_a|^{a+1} + \frac{\gamma(1-\omega)}{2}\phi_a^2 \\ &\quad + \frac{\alpha(1-\omega)}{2}y_2^2\end{aligned}\quad (20)$$

Obviously, $V(t) \geq 0$ and along the closed-loop trajectories, we have

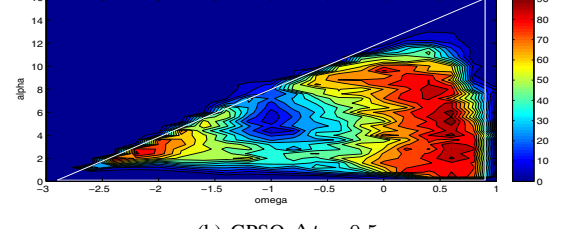
$$\begin{aligned}\frac{dV(t)}{dt} &= \beta(1-\omega)\text{sig}(\phi_a)^a \dot{\phi}_a + \gamma(1-\omega)\phi_a \dot{\phi}_a \\ &\quad + \alpha(1-\omega)y_2 \dot{y}_2 \\ &= -(1-\omega)^2(\gamma\phi_a + \beta\text{sig}(\phi_a)^a)^2\end{aligned}\quad (21)$$

Given initial state $y_1(0)$ and $y_2(0)$, if there exists $k > 0$ such that

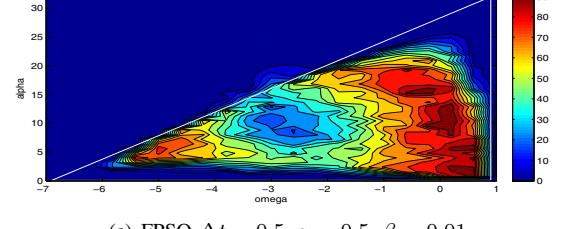
$$\frac{dV(t)}{dt} \leq -kV(t)^{\frac{2a}{a+1}}$$



(a) PSO



(b) GPSO $\Delta t = 0.5$



(c) FPSO $\Delta t = 0.5, \gamma = 0.5, \beta = 0.01$

Fig. 9. Success rates for the Rastrigin function for PSO, GPSO, and FPSO.

By lemma 1, $V(t)$ will reach zero in finite-time $t^* = \frac{(1+a)V(0)^{\frac{1+a}{1-a}}}{k(1-a)}$, which implies that $y_1(t)$ and $y_2(t)$ will be zero.

Suppose that $V(t) \neq 0$. Let $\Upsilon_1 = -\frac{\frac{dV(t)}{dt}}{V(t)^{\frac{2a}{1+a}}}$. Therefore,

$$\begin{aligned}\Upsilon_1 &= \frac{(1-\omega)^2(\gamma\phi_a + \beta\text{sig}(\phi_a)^a)^2}{\left[\rho_1|\phi_a|^{a+1} + \rho_2\phi_a^2 + \rho_3y_2^2\right]^{\frac{2a}{1+a}}} \\ &\geq \frac{(1-\omega)^2(\gamma\phi_a + \beta\text{sig}(\phi_a)^a)^2}{\rho_1^{\frac{2a}{1+a}}|\phi_a|^{2a} + \rho_2^{\frac{2a}{1+a}}|\phi_a|^{\frac{4a}{1+a}} + \rho_3^{\frac{2a}{1+a}}|y_2|^{\frac{4a}{1+a}}} \\ &\geq \frac{(1-\omega)^2\beta^2|\phi_a|^{2a}}{\rho_1^{\frac{2a}{1+a}}|\phi_a|^{2a} + \rho_2^{\frac{2a}{1+a}}|\phi_a|^{\frac{4a}{1+a}} + \rho_3^{\frac{2a}{1+a}}|y_2|^{\frac{4a}{1+a}}} \\ &\triangleq \Upsilon_2(y_1, y_2)\end{aligned}$$

where $\rho_1 = \frac{\beta(1-\omega)}{a+1}$, $\rho_2 = \frac{\gamma(1-\omega)}{2}$, and $\rho_3 = \frac{\alpha(1-\omega)}{2}$; The second inequality follows from the fact that $\phi_a = \text{sig}(\phi_a)$.

Let $\chi = \{\zeta \in \mathbb{R}^2 : \frac{1}{\max\{1-\omega, \alpha\}} \leq \|\zeta\|_\infty \leq \|\zeta(0)\|_\infty\}$ where $\|\cdot\|_\infty$ is the maximum norm. If $\chi \neq \emptyset$, then it is compact, and for any $[y_1, y_2]^T \in \chi$, $\Upsilon_2(y_1, y_2) \neq 0$. Hence, $k_1 = \min_{[y_1, y_2]^T \in \chi} \Upsilon_2(y_1, y_2)$ exists, and is larger than zero. On the other hand, if $\chi = \emptyset$, we have $0 < \|[y_1, y_2]^T\|_\infty <$

$\frac{1}{\max\{1-\omega, \alpha\}}$, i.e., $0 < |\phi_a| < 1$ such that

$$\Upsilon_2(y_1, y_2) > \frac{\beta^2(1-\omega)^2}{\rho_0} \frac{|\phi_a|^{2a}}{2|\phi_a|^{2a} + |y_2|^{\frac{4a}{1+a}}}$$

where $\rho_0 = \max\{\rho_1^{\frac{2a}{1+a}}, \rho_2^{\frac{2a}{1+a}}, \rho_3^{\frac{2a}{1+a}}\}$. Moreover, there exists a constant $k_2(\omega, \alpha)$ that satisfies $|y_2|^{\frac{2}{1+a}} < k_2|\phi_a|$. Hence,

$$\begin{aligned} \Upsilon_2(y_1, y_2) &> \frac{\beta^2(1-\omega)^2}{\rho_0} \frac{|\phi_a|^{2a}}{2|\phi_a|^{2a} + k_2|\phi_a|^{2a}} \\ &= \frac{\beta^2(1-\omega)^2}{\rho_0(2+k_2)} \end{aligned}$$

Let $k = \min\{k_1, \frac{\beta^2(1-\omega)^2}{\rho_0(2+k_2)}\}$. The step 2 is finished. Since $V(t)$ is radially unbounded and $\dot{V}(t)$ is negative definite, global stability holds. \square

For the discrete-time model of the FPSO algorithm, a conservative convergence region will be given in the following without the proof due to page limits.

$$\begin{aligned} \Omega_d &= \{(\omega, \alpha, a, \gamma, \beta) : 1 - \frac{2}{\Delta t \gamma} < \omega < 1, \\ &0 < \alpha < \frac{2\Delta t \gamma(\omega - 1) + 4}{\gamma \Delta t^2}, \\ &0 < a < 1, 0 < \gamma \leq 1, \\ &0 < \beta < \frac{0.01\gamma}{\Delta t^2(1-\omega)^a}\} \end{aligned} \quad (22)$$

Remark 2: The above convergence region (22) only shows that the proposed discrete FPSO algorithm will converge to an equilibrium within a finite-time interval. But the equilibrium may be an optimum or not. It should be pointed out that the parameters β and γ can improve the exploring and exploiting ability of the proposed discrete FPSO algorithm (see III-B). As a consequence, the proposed discrete FPSO algorithm can find the optimum with a higher success rate.

V. SIMULATION RESULTS

In this section, we will illustrate the performance capabilities of the proposed FPSO algorithm through three benchmark functions and the problem of the odor source localization.

A. Benchmark Functions

In this subsection, we will run several numerical simulations in order to test the performance capabilities of the proposed discrete-time FPSO algorithm. Three benchmark functions with two dimensions including Griewank, Rastrigin, and Ackley which belong to a type of ill-posed optimization problems (global minimum surrounded by multiple minima), will be used. A similar analysis has been done for the PSO case and the GPSO case [7], [9]. During the simulations, the max function evaluation is limited to 4000 (the population size is 40). In terms of the values of the parameters ω and α that satisfy the stability region of the corresponding algorithms (see triangles of Fig.8, Fig.9, and Fig.10; PSO algorithms $0 < \alpha < 4$, $-1 < \omega < 1$; CPSO algorithms $0 < \alpha < 16$, $-3 < \omega < 1$; FPSO algorithms $0 < \alpha < 32$, $-7 < \omega < 1$) the success rates over 100 simulations (within a tolerance of

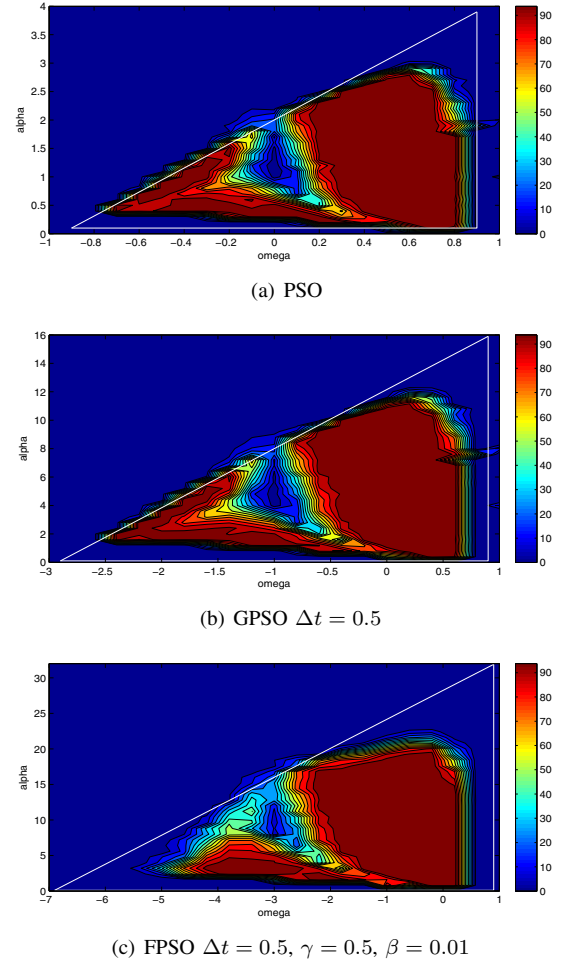


Fig. 10. Success rates for the Ackley function for PSO, GPSO, and FPSO

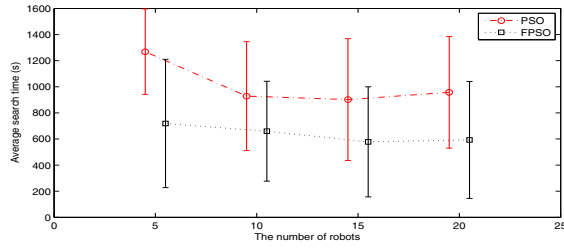
10^{-4}) are shown in Fig.8, Fig.9, and Fig.10 for Griewank, Rastrigin, and Ackley respectively.

From Fig.8, Fig.9, and Fig.10, one can see that the convergence region of the discrete-time FPSO algorithm increases in size due to the impact of the parameter γ and the best parameters move towards decreasing inertia and increasing accelerations. Moreover, one can also see that the proposed discrete-time FPSO algorithm can obtain the higher success rates within a wider range of parameters. Hence, the discrete-time FPSO algorithm provides a **flexible mechanism of parameter choice** to obtain the better results.

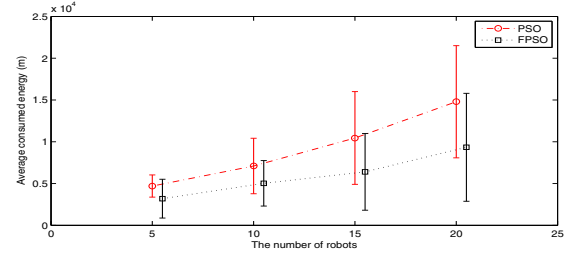
B. Odor Source Localization

The problem of odor source localization has been described in [11]. The readers can refer to [11] and the references therein. In this subsection, we will compare the search efficiency of the multi-robot system coordinated by the proposed continuous-time FPSO algorithm given in (14) with the continuous-time PSO algorithm stated in (4). Moreover, we adopt an odor model, proposed by [6], to establish a simulation environment which parameters are the same as those used in [11].

Table I shows the success rates based on 50 runs and Figure



(a) The average search time based on 50 runs



(b) The average consumed energy based on 50 runs

Fig. 11. The results of the problem of odor source localization for the continuous PSO algorithm ($\omega = 0.2, \alpha = 8$, the parameters are set based on the numerical simulation results that are not listed due to page limits) and the continuous FPSO algorithm ($\omega = -0.2, \alpha = 16, \beta = 0.01, \gamma = 0.5$)

TABLE I
THE SUCCESS RATES (%) BASED ON 50 RUNS

Algorithms	5 robots	10 robots	15 robots	20 robots
PSO	54	78	72	74
FPSO	76	92	90	88

11 (a) illustrates search time for the continuous-time PSO and FPSO algorithms. Moreover, since path length denotes the energy consumed by robots, the shorter path length means the better search performance. From Fig.11 (b), one can see that robots coordinated by the continuous-time FPSO algorithm consume the lesser energy than those coordinated by the continuous-time PSO algorithm.

VI. CONCLUSION

A finite-time particle swarm optimization (FPSO) algorithm has been proposed. Two versions of the FPSO algorithm: the continuous-time FPSO algorithm and the discrete-time FPSO algorithm have been given. For the continuous-time FPSO algorithm, we have introduced a nonlinear damping item and a parameter into the continuous model of the PSO algorithm such that the continuous-time FPSO algorithm can converge within a finite-time interval and its exploration capability can be improved. For the discrete-time FPSO algorithm, we have used the same discretization scheme as the GPSO algorithm to derive it. Moreover, we have used the Lyapunov approach to analyze the convergence of the continuous-time FPSO algorithm and given a stability region of the discrete-time FPSO algorithm. Finally, this study has shown the performance capabilities of the proposed FPSO algorithm through numerical simulations on the benchmark functions and the problem of odor source localization.

ACKNOWLEDGEMENT

The research work of Q.-L. Han was supported in part by the Australian Research Council Discovery Projects under Grant DP1096780 and Grant DP0986376, and the Research Advancement Awards Scheme Program (January 2010 - December 2012) and the RDI Merit Grant Scheme Project under Grant RDIM1109 (January 2011 - December 2011) at Central Queensland University, Australia. The research work of Q. Lu

was supported by the Natural Science Foundation of Zhejiang Province, China, under Grant Y1090426 and Grant Y1100954.

REFERENCES

- [1] S. P. Bhat and D. S. Bernstein, "Finite-time stability of continuous autonomous systems," *SIAM Journal of Control and Optimization*, vol. 38, no. 3, pp. 751–766, 2000.
- [2] M. Clerc and J. Kennedy, "The particle swarm-explosion, stability and convergence in a multidimensional complex space," *IEEE Transactions on Evolutionary Computation*, vol. 6, no. 2, pp. 58–73, February 2002.
- [3] J. Cortés, "Finite-time convergent gradient flows with applications to network consensus," *Automatica*, vol. 42, no. 11, pp. 1993–2000, 2006.
- [4] I. D. Couzin, J. Krause, N. R. Franks, and S. A. Levin, "Effective leadership and decision-making in animal groups on the move," *Nature*, vol. 433, pp. 513–516, February 2005.
- [5] R. C. Eberhart and Y. Shi, "Parameter selection in particle swarm optimization," in *Proceedings of the 7th International Conference on Evolutionary Programming*, San Diego, CA, USA, 1998, pp. 591–600.
- [6] J. A. Farrell, J. Murlis, X. Z. Long, W. Li, and T. Ring, "Filament-based atmospheric dispersion model to achieve short time-scale structure of odor plumes," *Environment Fluid Mechanics*, vol. 2, no. 1-2, pp. 143–169, 2002.
- [7] J. L. Fernández-Martínez and E. García-Gonzalo, "The generalized pso: A new door to pso evolution," *Journal of Artificial Evolution and Applications*, vol. 2008, pp. 1–15, 2008.
- [8] J. L. Fernández-Martínez and E. García-Gonzalo, "Stochastic stability analysis of the linear continuous and discrete pso models," *IEEE Transactions on Evolutionary Computation*, vol. 15, no. 3, pp. 405–423, June 2011.
- [9] J. L. Fernández-Martínez, E. García-Gonzalo, and J. P. Fernández-Alvarez, "Theoretical analysis of particle swarm trajectories through a mechanical analogy," *International Journal of Computational Intelligence Research*, vol. 4, no. 2, 2008.
- [10] V. Kadiramanathan, K. Selvarajah, and P. J. Fleming, "Stability analysis of the particle dynamics in particle swarm optimizer," *IEEE Transactions on Evolutionary Computation*, vol. 10, no. 3, pp. 245–255, June 2006.
- [11] Q. Lu and Q.-L. Han, "A distributed coordination control scheme for odor source localization," in *Proceedings of the 36th Annual Conference of the IEEE Industrial Electronics Society*, Phoenix, AZ, USA, 2010, pp. 1413–1418.
- [12] R. Mendes, J. Kennedy, and J. Neves, "The fully informed particle swarm: Simpler maybe better," *IEEE Transactions on Evolutionary Computation*, vol. 8, no. 3, pp. 204–210, June 2004.
- [13] R. Olfati-Saber, "Flocking for multi-agent dynamic systems: Algorithms and theory," *IEEE Transactions on Automatic Control*, vol. 51, no. 3, pp. 401–420, March 2006.
- [14] M. Wachowiak, R. Smolikova, Y. Zheng, and A. Elmaghraby, "An approach to multimodal biomedical image registration utilizing particle swarm optimization," *IEEE Transactions on Evolutionary Computation*, vol. 8, no. 3, pp. 289–301, June 2004.
- [15] F. Xiao, L. Wang, J. Chen, and Y.-P. Gao, "Finite-time formation control for multi-agent systems," *Automatica*, vol. 45, no. 11, pp. 2605–2611, 2009.